J. Plasma Fusion Res. SERIES, Vol.7 (2006) 54-58

On the Anomalous Characteristics in the P and R Branches in a Hydrogen Fulcher Band

KADO Shinichiro, YAMASAKI Daisuke[1], XIAO Bingjia[2], IIDA Yohei[1],
OKAMOTO Atsushi*, KAJITA Shin[1**], SHIKAMA Taiichi[1],
OISHI Tetsutaro[1] and TANAKA Satoru[1]

High Temperature Plasma Center, The University of Tokyo, Chiba 227-8568, Japan

[1] *Graduate School of Engineering, The University of Tokyo, Tokyo 113-8656, Japan*

[2] *Chinese Academy of Sciences, Hefei, Anhui 230031, China*

(Received: 4 October 2004 / Accepted: 24 May 2005)

Abstract

Anomalous characteristics in the P and R branches in hydrogen Fulcher-α emissions were investigated with respect to rotational temperature and population in the excited electronic state (upper-Fulcher state). The ro-vibrational population distribution of the ground electronic state was deduced by applying the coronal equilibrium to the Q branch, and then the population for the P and R branches was predicted. The anomalies in P and R branches can be found in the rotational temperature and the branching ratio between the branches. Our results suggest that the sum of the emission from P and R branches seems to agree with that predicted based on the Q branch emission.

Keywords:

Fulcher band, intensity anomaly, hollow cathode discharge, rotational structure, vibrational temperature, rotational temperature

1. Introduction

Fulcher-α band ($d^3\Pi_u^- - a\Sigma_g^+$) spectra are widely used to measure ro-vibrational distribution of the hydrogen molecules in divertor plasmas in fusion devices [1], divertor plasma simulators [2], and laboratory plasmas [3], including negative ion sources [4]. Because it has been known, from the early stage of molecular spectroscopy, that the P and R branches, which originate in the $d^3\Pi_u^+$ sublevel, exhibit anomalous intensity compared to the Q branch, which originates in $d^3\Pi_u^-$ [5], usually only the Q branch has been used to determine the ro-vibrational distribution in the ground electronic state. The reason for this phenomenon has often been referred to as the perturbation between $d^3\Pi_u^+$ and $e^3\Sigma_u^+$ [6,7]. However, if the characteristic can be clarified either theoretically or empirically, data points of the Fulcher band could be increased, and then a better fit to obtain the ro-vibrational structure of the ground electronic state could be provided.

In this study, we investigated the P, Q, and R branches in the diagonal Fulcher-α transition using the hollow cathode glow discharge of 230 V – 70 mA.

2. Principle of the diagnostics

We have developed an analysis scheme in which the ground state ($X^1\Sigma_g^+$) populations for both vibrational (v) and rotational (J) distributions are assumed to be described by the Boltzmann temperatures T_{vib}^X and T_{rot}^X, respectively. The electron impact excitation rate from the $X(v, J)$ state to the $d(v', J')$ state, $R_{XvJ}^{dv'J'}$, and the spontaneous emission coefficient from the $d(v', J')$ state to the $a(v'', J'')$ state, $A_{av''J''}^{dv'J'}$, are used in a coronal model to determine T_{vib}^X and T_{rot}^X. Then, the measured intensity ratio of the Fulcher band spectra is fitted to the function [2],

$$I_{av''J''}^{dv'J'} = \frac{hc}{\lambda_{av''J''}^{dv'J'}} \frac{A_{av''J''}^{dv'J'}}{\sum_{v'',J''} A_{av''J''}^{dv'J'}} \times n_e \sum_{v,J} \left\{ R_{XvJ}^{dv'J'} C_v (2J+1) g_{as}^J \exp\left[-\frac{F_X(J,v)}{kT_{rot}^X} - \frac{G_X(v) - G_X(0)}{kT_{vib}^X} \right] \right\}, \quad (1)$$

where $\lambda_{av''J''}^{dv'J'}$ is the wavelength of the measured line; $F_X(J, v)$ and $G_X(v)$ are the rotational and vibrational energies in the $X^1\Sigma_g^+$ state, respectively; h and c are the

Corresponding author's e-mail: kado@q.t.u-tokyo.ac.jp
*Present affiliation: *Tohoku University, **Nagoya University*

Planck constant and the light velocity, respectively; and C_v is the normalization constant with respect to J for each v level. The degeneracy of nuclear spin g_{as}^J stands for "asymmetric" or "symmetric," depending on the symmetry of the level J. In H_2, levels of odd J in $d^3\Pi_u^-$ (Q branches) and $X^1\Sigma_g^+$ and of even J in $d^3\Pi_u^+$ (P and R branches) are asymmetric, so that the wave function of the nuclear spin is symmetric to satisfy the feature of fermions, i.e., $g_{as}^J = g_s^a = 3$, while the opposite case requires $g_{as}^J = g_a^s = 1$.

The ro-vibronic structure of $A_{av''J''}^{av'J'}$ for the diagonal band can be well described by Franck-Condon factor $q_{v'v''}$ and the Hönl-London factor for the P, Q, or R branch, namely,

$$S_{J'J''}^P = J'/2,$$
$$S_{J'J''}^Q = (2J'+1)/2,$$
$$S_{J'J''}^R = (J'+1)/2. \quad (2)$$

Note that $S_{J'J''}^Q = S_{J'J''}^P + S_{J'J''}^R = (2J'+1)/2.$ (3)

The ro-vibrational structure in the excitation rate $R_{XvJ}^{dv'J'}$ is evaluated from the adiabatic approximation combined with Gryzinski's semi-classical electron exchange cross-sections [8]:

$$R_{XvJ}^{dv'J'} = q_{Xv}^{dv'} < Q_{v'\leftarrow v}^{Gryzinski} v_e > a_{0J}^{1J'} \delta_{g_{as}^J}^{g'^J_{as}},$$

$$\sum_{K'} a_{\Lambda K}^{\Lambda' K'} = \sum_{K'} \sum_r \bar{Q}'_r (2K+1) \begin{pmatrix} K' & r & K \\ \Lambda' & \Lambda-\Lambda' & -\Lambda \end{pmatrix}^2 = 1, \quad (4)$$

where $\bar{Q}'_r$ is the multi-polar components of the partial cross-section determined in Ref. [9], which, for $r = 1 \sim 4$, are 0.76, 0.122, 0.1, and 0.014. Note that the dipolar component of $a_{0J}^{1J'}$, namely $\bar{Q}'_1$ with $r = 1$, corresponds to the Hönl-London factor for the X to d transition. Kronecker's delta represents the selection rule for the symmetry of nuclear spin. The spin multiplicity is so small that K can be replaced by J in this case.

For the purpose of comparing the accuracy of the fitting, we executed a Boltzmann plot of the $d^3\Pi_u^-$ or $d^3\Pi_u^+$ state. Although the rotational distribution of the excited vibronic state is not necessarily in thermal equilibrium, lower rotational levels are well described by $T_{rot}^{dv'}$, which is dependent on v'.

3. Experimental results

Plasma was generated in a hollow cathode discharge chamber [10]. The cathode region was 19 mm in diameter. The discharge current and voltage were 70 mA and 230 – 270 V, respectively. The operating range of the gas pressure was 10 – 300 Pa in our present apparatus. The typical electron density, n_e, and temperature, T_e, were 10^9 cm^{-3} and a few eV, respectively.

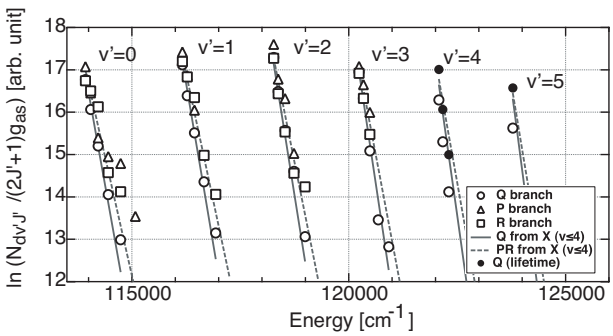

Fig. 1 Molecular Boltzmann plot of the Fulcher band in hollow cathode discharge at 110 Pa. Solid lines represent the reconstruction from the fitting result of T_{rot} and T_{vib} in the ground electronic state using the data for $v' \leq 3$. Filled circles represent the corrected data for the Q branch, taking the relative lifetime into account.

A 1-m Czerny-Turner scanning monochromator equipped with a 2400 grooves/mm holographic grating and a photo-multiplier tube detector (PMT: Hamamatsu R928) was used for the optical measurements. The typical wavelength resolution in the present work was less than 0.03 nm at a 50-μm slit width.

We measured n_e and T_e at the center of the hollow cathode using a Langmuir probe made of Molybdenum and covered with a Pyrex glass rod. In the present study, the working gas pressure was set to 110 Pa. The n_e and T_e were 3.9×10^9 cm^{-3} and 3.9 eV, respectively.

Molecular Boltzmann plots of $d^3\Pi_u^{+/-}$ states population are shown in Fig. 1. Hönl-London factors for P, Q, and R branches were used. Q branch spectra of $v' \leq 3$ were normally used for the evaluation of T_{vib}^X and T_{rot}^X. Obtained results were $T_{vib}^X = 2301 \pm 292$ K and $T_{rot}^X = 380.4 \pm 21.7$ K. Reconstructed distributions of the $d^3\Pi_u^{+/-}$ states using these fitting results are also shown (lines). The intensity of $v' \geq 4$ is weaker, since the dissociation limit to H(1s) and H(2s) lies between the $v' = 3$ and 4 levels (open circles). The filled circles in $v' \geq 4$ represent the corrected data by applying the lifetime of the state involved in vacuum. One can see that corrected values are slightly higher in this condition, which is discussed later.

The so-called anomaly in the P and R branches cannot be compensated for by the lifetime [10]. As seen in the figure, the anomaly in the P and R branches consists in the differences in (1) the rotational temperature of the $d^3\Pi_u^+$ state, and (2) the population.

For the purpose of investigating the characteristics of the anomaly, we evaluated T_{vib}^X and T_{rot}^X from the Q branch, predicted the populations of $d^3\Pi_u^+$, and then compared them with the P and R branch emission in

terms of $T_{rot}^{dv'}$ and the population.

4. Discussion

4.1 Rotational temperature

In Fig. 2, $T_{rot}^{dv'}$, deduced from the Boltzmann plot method for $d^3\Pi_u^{+/-}$ states, is shown as a function of v' (markers) together with the calculated values from the fitted T_{rot}^X and T_{vib}^X to the Q branch spectra (lines). The data in Fig. 1 were used. There are considerable discrepancies between branches. In particular, the adiabatic approximation requires that P and R branches from the same Λ-sublevel provide equal values.

There have been experiments to determine T_{rot}^X, which can be interpreted as the gas temperature in a high-temperature regime from the obtained rotational temperature in the $d^3\Pi_u^-$ state for a specific v' level, $T_{rot}^{dv'}$. The most commonly used formula for the Q branch was proposed by Lavrov [12], as follows:

$$\frac{T_{rot}^X(v=0)}{B_{v=0}^X} \sim \frac{T_{rot}^d(v')}{B_{v'}^d}, \qquad (5)$$

where $B_{v=0}^X$ and $B_{v'}^d$ denote the rotational constants, which are 59.3 and 29.6 ($v' = 0$) cm^{-1}, respectively. Hence $T_{rot}^X(v=0) \sim 2T_{rot}^d(v'=0)$.

However, our model based on eq. (4) gives different values, especially in a low T_{rot}^X regime, as shown in Fig. 3. The difference comes from the multi-polar components of $\bar{Q}_r'$. The dipole component, $r = 1$, provides the Hönl-London factor. Due to the selection rule with respect to the symmetry of the nuclear spin, rotational quanta do not change in either the excitation to $d^3\Pi_u^-$ or in the radiative decay to $a^3\Sigma_g^+$ for the Q branch. Consequently, the Boltzmann distribution in the rotational population conserves between the vibronic states, which yields eq. (5), shown in the line without markers

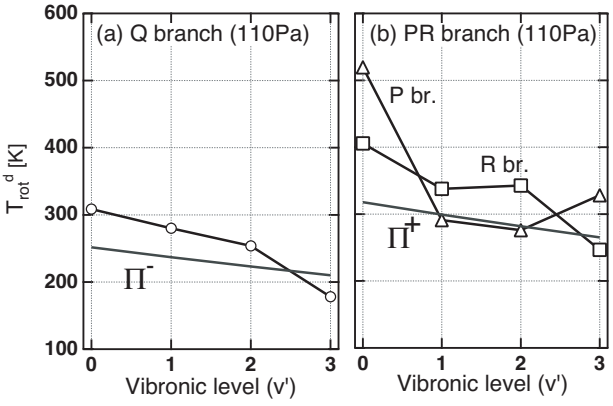

Fig. 2 Rotational temperature in the (a) $d^3\Pi_u^-$ and (b) $d^3\Pi_u^+$ state as a function of the vibronic level v'. Lines without markers are the reconstructed values from the fitting result of T_{rot} and T_{vib} in the ground electronic state.

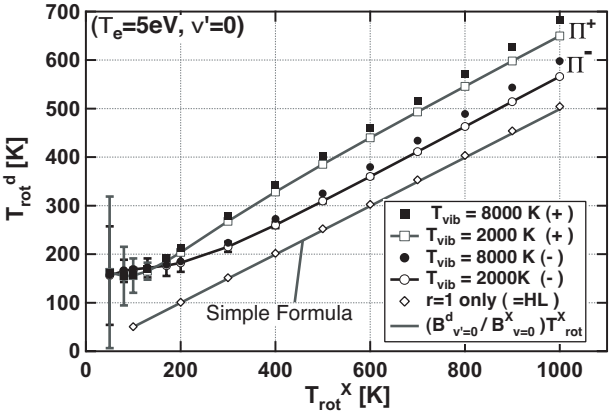

Fig. 3 Relation between (X, $v=0$) and (d, $v'=0$) state rotational temperatures. Results based on the simple linear formula [12] and those based on the dipolar component of the excitation rate are added as a comparison.

in Fig. 3.

Open diamonds represent the result using $r = 1$ only. This calculation agrees with the simple formula. By taking the higher multi-polar components into account, however, this conservation breaks. For example, $J' = 1$ in $d^3\Pi_u^-$ (ortho-H_2) is populated by the odd J levels in $X^1\Sigma_g^+$, while $J' = 1$ in $d^3\Pi_u^+$ (para-H_2) is populated by the even J levels. Consequently, the relation in low T_{rot}^X becomes non-linear. The large error-bars in the lower T_{rot}^X are due to the fact that the excited state distribution cannot be described by the Boltzmann temperature. In the same manner, the multi-polar components make the $d^3\Pi_u^-$ state rotational distribution slightly depart from Boltzmann. This might be the dominant reason for the difference between the Boltzmann plot and the calculated values seen in Fig. 2. Thus, the above simple evaluation cannot apply. In other words, it is important to consider the multi-polar components in determining T_{rot}^X and to use curves such as those in Fig. 3 obtained from the model, or more desirably, to determine the best-fitted T_{rot}^X to a whole Fulcher band structure based on the model provided here in eq. (1).

Deduced $T_{rot}^{dv'}$ does not depend on T_e and has only a slight dependence on T_{vib}^X(ignorable). It should be noted, however, that by considering the multi-polar components, $T_{rot}^{dv'}$ in $d^3\Pi_u^-$ and $d^3\Pi_u^+$ become slightly different to each other[1]. However, the predicted $T_{rot}^{dv'}$ in $d^3\Pi_u^+$ cannot reproduce the experimental data. This result indicates that the adiabatic approximation cannot be applied in the analysis of the rotational structure of P and R branches.

[1] Fig. 5 (b) in Ref. [10] had an error in $T_{rot}^{dv'}$ of $d^3\Pi_u^+$, which was corrected here.

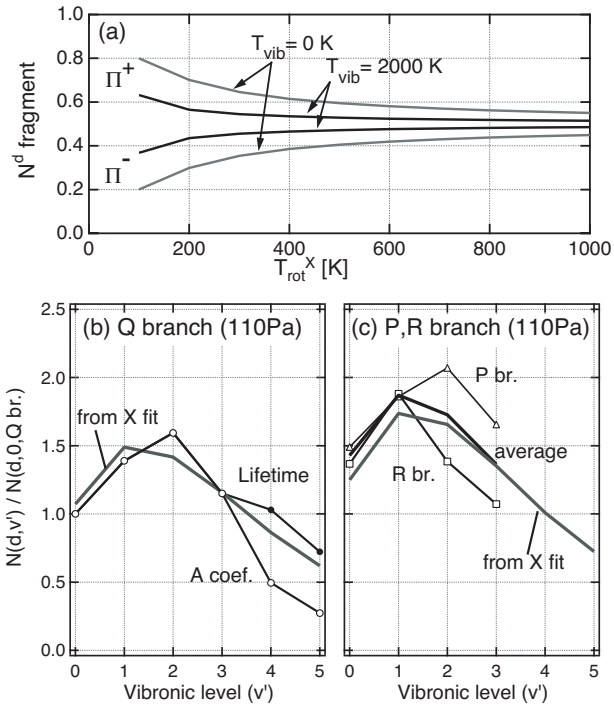

Fig. 4 (a) Calculated portion of the population density of $d^3\Pi_u^-$ and $d^3\Pi_u^+$ states as a function of rotational temperature in the X state for the vibrational temperature of 0 and 2000 K. (b) Population summed over the rotational structure of the vibronic states normalized to that of $v'=0$ of the Q branch. (c) Same plot as (b) for the P and R branches.

4.2 Population density of the Λ-type doublet states

According to the selection rule, the lowest rotational level in $X^1\Sigma_g$(para-H_2) can be excited mainly to $J'=1$ in $d^3\Pi_u^+$. Consequently, $d^3\Pi_u^+$ has more population than $d^3\Pi_u^-$ in low-density coronal equilibrium plasmas where collisional redistribution of the Λ-doublet state is negligible. A collisional-radiative equilibrium including the other electronic states may tend to distribute the population proportional to the statistical weight again. Therefore it is especially important to consider the unbalance of the excitation fluxes when investigating the intensity ratio from the Λ-doublet in low-density plasmas.

The calculated ratio of populations in the $d^3\Pi_u^-$ to $d^3\Pi_u^+$ states as a function of T_{rot}^X is shown in Fig. 4(a). The ratio does not depend on T_e, while weak dependence on T_{vib}^X can be seen. The difference between the Λ-doublet states is more apparent in the low T_{rot}^X and T_{vib}^X regime.

In Fig. 4 (b) and 4 (c), the population in $d^3\Pi_u^{+/-}$ states deduced from the experimental data for 110 Pa are shown together with the reproduced population from fitted T_{rot}^X and T_{vib}^X. The population for each v' level was evaluated by the Boltzmann plot to obtain $T_{rot}^{dv'}$, and then the resultant rotational population was summed up to $J'=20$. Because we applied lifetimes in vacuum relative to that for $v' \leq 3$, over-estimation occurred for the corrected vibronic population in $v'=4$ and 5 in the Q branch. This correction reproduces the population without taking the predissociation process into consideration. Collisions to the neutral could shorten the lifetime for $v \leq 3$. In fact, this correction scheme shows better results in the case of 15 Pa [10]. This should be confirmed in a future study.

There is an obvious discrepancy between the cases of the P and R branches. However, the average of these branches coincides with the reproduced population. This suggests that the anomaly consists in the branching ratio of the P and R branches. In this respect, intensity perturbation caused by the adjacent electronic state is not obvious, though the rotational temperature exhibits an anomaly. This tendency was also found in the different discharge condition of 15 Pa and the reanalyzed historical data of Ginsburg [5].

5. Summary

In Fulcher-α band spectra, populations of the vibronic state $v' \leq 4$ in the Q branch can be corrected to some extent by taking into account the lifetime of the states. The 110 Pa case in comparison with our previous result at 15 Pa indicates that the collisional de-excitation of the $d^3\Pi_u^-$ might be taken into account. The ratio of P and R branch intensities is far from that expected from the Hönl-London formulae. The anomaly is also found in the fact that the rotational temperatures in $d^3\Pi_u^+$ deduced from the P and R branches are different from each other. However, our initial results show that the average of the upper-Fulcher populations in the vibronic state deduced from the P and R branches coincides with the population predicted from the Q branch by taking into consideration the difference in the selection rule of excitation from the ground electronic state based on the adiabatic approximation.

Acknowledgements

This work was supported in part by NIFS cllaborative research program (NIFS04KDAB009).

References

[1] U. Fantz and B. Heger, Plasma Phys. Control. Fusion **40**, 2023 (1998).

[2] B. Xiao, S. Kado, S. Kajita and D. Yamasaki, Plasma Phys. Control. Fusion **46**, 653 (2004).

[3] B.P. Lavrov *et al.*, Plasma Source Sci. Technol. **12**, 576 (2003).

[4] E. Surrey and B. Crowley, Plasma Phys. Control. Fusion **45**, 1209 (2003).

[5] N. Ginsburg and G.H. Dieke, Phys. Rev. **59**, 632

(1941).

[6] H. Lefebvre-Brion and R.W. Field, *Perturbations in the Spectra of Diatomic Molecules* (Academic, New York, 1986).

[7] T. Kiyoshima and H. Sato, Phys. Rev. A **48**, 4771 (1993).

[8] M. Gryzinski, Phys. Rev. **138**, A336 (1965).

[9] N.N. Sobolev, *Electron-excited molecules in non-equilibrium plasma* (NewYork, Nova Science Publishers, 1989), pp. 121-173.

[10] S. Kado, D. Yamasaki, Y. Iida and B. Xiao,J. Plasma Fusion Res. **80**, 783 (2004) [in Japanese].

[11] S.A. Astashkevich *et al*., J. Quant. Spectrosc. Radiat. Transf. **56**, 725 (1996).

[12] B.P. Lavrov, V.N. Ostrovsky and V.I. Ustimov, J. Phys. B **14**, 4701 (1981).